

Scattering and extinction of evanescent waves by small particles

M. Quinten, A. Pack, R. Wannemacher

Institut für Physik, Technische Universität Chemnitz, D-09107 Chemnitz, Germany

Received: 14 May 1998/Revised version: 31 July 1998

Abstract. Expressions have been obtained for the total cross sections for extinction and scattering of evanescent waves by small spherical particles. Due to the different structure of p- and s-polarized waves, cross sections for both extinction and scattering of p-polarised evanescent waves exceed those for s-polarised waves, as long as the Mie coefficients for magnetic multipoles are smaller than those for electric multipoles for each multipolar order, i.e. for sufficiently small particles. The difference increases with the angle of incidence of the totally reflected wave. The definition of cross sections for evanescent-wave excitation with variable intensity over the cross-sectional area of the particle allows quantitative comparison with the case of plane-wave excitation. For example, within the dipole approximation the cross sections for plane-wave excitation lie between those for p- and s-polarised evanescent-wave excitation, respectively. Due to the inhomogeneity of the evanescent field higher multipole contributions are strongly enhanced as compared to plane-wave excitation and increase further with the angle of incidence, resulting in corresponding changes in the scattering and extinction spectra. These effects are demonstrated in the specific case of scattering of evanescent waves by small silver particles.

PACS: 42.25.Fx; 78.40.-q

Since the early work of Gustav Mie [1] on the scattering of electromagnetic waves by small spherical particles extensive use has been made of Mie's theory and later extensions thereof to determine the size, shape, and orientation of small particles in vacuum or in gaseous, liquid, or solid media. Scientists and engineers from a large variety of disciplines – physics, electrical engineering, meteorology, chemistry, biophysics, and astronomy – are concerned with this field.

Whereas in standard experimental setups for such investigations usually large ensembles of scattering particles are investigated, the recent development of a near-field optical microscope, employing scattering of an evanescent wave at a nanometer-sized tip interacting with the sample [2, 3], has

yielded spatial resolution in the 1-nm range, i.e. far beyond the diffraction limit of conventional optical microscopes. The wide potential applications of such a scattering microscopy and spectroscopy, especially in biology, medicine, materials science, and information technology have motivated us to reconsider scattering and extinction of evanescent waves by small particles. Although the basic formulae for Mie scattering of evanescent waves result from analytic continuation of the standard case of plane-wave excitation, the cross sections and scattered power seem not to have been discussed thoroughly for evanescent waves, and several aspects seem to have been overlooked in the literature. As early as 1979 Chew et al. [4] started to discuss scattering of evanescent waves by spherical particles. Their theory was recently slightly corrected by Liu et al. [5]. However, as these authors were only interested in the differential scattering cross sections of relatively large particles, which were computed numerically from analytical expressions for the scattered fields, we have calculated total cross sections for evanescent-wave excitation and discuss in this paper their dependence on wavelength, angle of incidence, and particle sizes.

The paper is organized as follows. In Sect. 1 we briefly repeat the theory of evanescent-wave scattering and calculate total cross sections from Poynting's law by normalizing to the total power incident on the particle. To this end we give an expression for the normalization integral in the case of evanescent-wave excitation, which varies over the particle cross section. In Sect. 2 we present analytical results for small silver particles and compare them to results obtained with the numerical multiple multipole (MMP) method. The latter is used to study the additional effect of multiple scattering at the prism surface. Finally, in Sect. 3 a summary of the results is given.

1 Theory of evanescent wave scattering by spheres

Chew et al. [4] outlined the theory for scattering of evanescent waves by a spherical particle, which essentially consists in the

analytical continuation of the case of plane-wave excitation to complex angles of incidence. In the following we briefly repeat the formulae necessary for the derivation of total cross sections. We assume a spherical particle in front of a glass prism of refractive index n_p within a medium of real refractive index n_M at distance d from the prism surface (Fig. 1). Multiple scattering at the particle and prism surfaces is neglected at this point. A plane wave propagating in the prism and incident at a subcritical angle θ_i gets partly reflected and partly refracted at the boundary glass–air, the refraction being described by Snell’s law. In the reference frame of the particle the refracted wave is incident at angle θ_k to the z axis, as given by Snell’s law.

The electric field of the refracted wave may be written as

$$\mathbf{E} = E_t \mathbf{e}_t \exp[ik_M(z \cos \theta_k + x \sin \theta_k)], \quad (1)$$

with the polarization vector $\mathbf{e}_t = \mathbf{e}_y$ for the case of s-polarisation, and $\mathbf{e}_t = (\cos \theta_k, 0, -\sin \theta_k)^T$ for p-polarisation, and $k_M = \frac{\omega}{c} n_M$. E_t is the complex magnitude of the electric field vector of the refracted wave, which is determined using Fresnel’s equations. This wave is expanded in spherical coordinates into electric and magnetic multipoles as usual. For the general case $\theta_k \neq 0$ contributions of polynomials P_{nm} with $m \neq \pm 1$ are obtained which are not required in standard Mie theory where $\theta_k = 0$:

$$\begin{aligned} \mathbf{E}_{\text{inc}}^{\text{s,p}} &= \sum_{n=1}^{\infty} \sum_{m=-n}^n \frac{ic}{n_M^2 \omega} \alpha_{\text{TM}}^{\text{s,p}}(n, m) [\nabla \times \mathbf{j}_n(\rho) \mathbf{X}_{nm}] \\ &\quad + \alpha_{\text{TE}}^{\text{s,p}}(n, m) [\mathbf{j}_n(\rho) \mathbf{X}_{nm}], \end{aligned} \quad (2a)$$

$$\begin{aligned} \mathbf{H}_{\text{inc}}^{\text{s,p}} &= \frac{1}{\mu_0 c} \sum_{n=1}^{\infty} \sum_{m=-n}^n \alpha_{\text{TM}}^{\text{s,p}}(n, m) [\mathbf{j}_n(\rho) \mathbf{X}_{nm}] \\ &\quad - \frac{ic}{\omega} \alpha_{\text{TE}}^{\text{s,p}}(n, m) [\nabla \times \mathbf{j}_n(\rho) \mathbf{X}_{nm}], \end{aligned} \quad (2b)$$

where $\mathbf{X}_{nm} = LY_{nm}$ are the well-known vector spherical harmonics and $\rho = k_M r$. The expansion coefficients are given

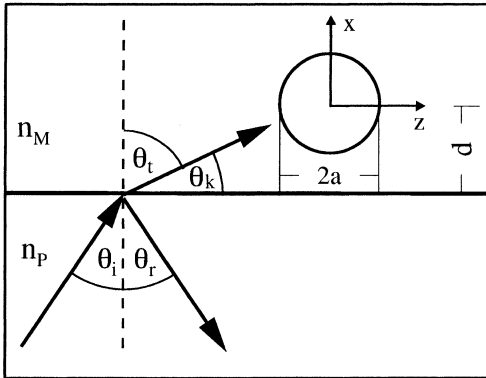


Fig. 1. Geometry of the scattering problem. The refractive indices n_p , n_M of the prism and of the medium surrounding the sphere, respectively, are assumed to be real

by [4]:

$$\begin{aligned} \alpha_{\text{TM}}^{\text{s}}(n, m) &= 2i^n n_M \left[\frac{\pi(2n+1)(n-m)!}{n(n+1)(n+m)!} \right]^{1/2} \\ &\quad \times \frac{m P_{nm}(\cos \theta_k)}{\sin \theta_k} E_t^{\text{s}}, \end{aligned} \quad (3a)$$

$$\begin{aligned} \alpha_{\text{TE}}^{\text{s}}(n, m) &= 2i^{n+1} \left[\frac{\pi(2n+1)(n-m)!}{n(n+1)(n+m)!} \right]^{1/2} \\ &\quad \times \frac{dP_{nm}(\cos \theta_k)}{d\theta_k} E_t^{\text{s}}, \end{aligned} \quad (3b)$$

$$\begin{aligned} \alpha_{\text{TM}}^{\text{p}}(n, m) &= 2i^{n+1} n_M \left[\frac{\pi(2n+1)(n-m)!}{n(n+1)(n+m)!} \right]^{1/2} \\ &\quad \times \frac{dP_{nm}(\cos \theta_k)}{d\theta_k} E_t^{\text{p}}, \end{aligned} \quad (3c)$$

$$\begin{aligned} \alpha_{\text{TE}}^{\text{p}}(n, m) &= -2i^n \left[\frac{\pi(2n+1)(n-m)!}{n(n+1)(n+m)!} \right]^{1/2} \\ &\quad \times \frac{m P_{nm}(\cos \theta_k)}{\sin \theta_k} E_t^{\text{p}}, \end{aligned} \quad (3d)$$

where the subscripts TM and TE stand for transverse magnetic and transverse electric modes and the superscripts s and p represent the polarization of the wave. For the scattered fields outside of the sphere a similar expansion may be set up.

$$\begin{aligned} \mathbf{E}_{\text{sca}}^{\text{s,p}} &= \sum_{n=1}^{\infty} \sum_{m=-n}^n \frac{ic}{n_M^2 \omega} \beta_{\text{TM}}^{\text{s,p}}(n, m) [\nabla \times \mathbf{h}_n^{(1)}(\rho) \mathbf{X}_{nm}] \\ &\quad + \beta_{\text{TE}}^{\text{s,p}}(n, m) [\mathbf{h}_n^{(1)}(\rho) \mathbf{X}_{nm}], \end{aligned} \quad (4a)$$

$$\begin{aligned} \mathbf{H}_{\text{sca}}^{\text{s,p}} &= \frac{1}{\mu_0 c} \sum_{n=1}^{\infty} \sum_{m=-n}^n \beta_{\text{TM}}^{\text{s,p}}(n, m) [\mathbf{h}_n^{(1)}(\rho) \mathbf{X}_{nm}] \\ &\quad - \frac{ic}{\omega} \beta_{\text{TE}}^{\text{s,p}}(n, m) [\nabla \times \mathbf{h}_n^{(1)}(\rho) \mathbf{X}_{nm}], \end{aligned} \quad (4b)$$

where the spherical Bessel functions $\mathbf{j}_n(\rho)$ have been replaced by spherical Hankel functions of first kind $\mathbf{h}_n^{(1)}(\rho)$, which for large arguments represent outgoing spherical waves. Using a similar expansion for the fields in the interior of the sphere (of which we will have no further need here) and applying Maxwell’s boundary conditions at the surface of the spherical particle results in the scattering coefficients of the sphere, given by

$$\beta_{\text{TM}}^{\text{s,p}}(n, m) = a_n \alpha_{\text{TM}}^{\text{s,p}}(n, m), \quad (5a)$$

$$\beta_{\text{TE}}^{\text{s,p}}(n, m) = b_n \alpha_{\text{TE}}^{\text{s,p}}(n, m), \quad (5b)$$

where a_n and b_n are the Mie coefficients. These equations coincide with those of [4], except for the signs in (3b,c) [6] and except that in the results for the scattering coefficients not the complex conjugates of the associated Legendre polynomials are used but their actual values. The necessity of the latter correction was already pointed out by Liu et al. [5].

Applying Poynting’s law for the absorbed power density in the stationary case we obtain the cross sections for extinc-

tion and scattering of the refracted plane wave.

For s-polarised light:

$$\sigma_{\text{ext}}^s = \frac{2\pi}{k_M^2} N^{-1} \operatorname{Re} \sum_{n=1}^{\infty} (2n+1) (a_n \Pi_n + b_n T_n), \quad (6a)$$

$$\sigma_{\text{sca}}^s = \frac{2\pi}{k_M^2} N^{-1} \sum_{n=1}^{\infty} (2n+1) \left(|a_n|^2 \Pi_n + |b_n|^2 T_n \right). \quad (6b)$$

For p-polarized light:

$$\sigma_{\text{ext}}^p = \frac{2\pi}{k_M^2} N^{-1} \operatorname{Re} \sum_{n=1}^{\infty} (2n+1) (a_n T_n + b_n \Pi_n), \quad (6c)$$

$$\sigma_{\text{sca}}^p = \frac{2\pi}{k_M^2} N^{-1} \sum_{n=1}^{\infty} (2n+1) \left(|a_n|^2 T_n + |b_n|^2 \Pi_n \right). \quad (6d)$$

The definitions are:

$$\Pi_n(\theta_k) = \frac{2}{n(n+1)} \sum_{m=-n}^n \frac{(n-m)!}{(n+m)!} \left| m \frac{P_{nm}(\cos \theta_k)}{\sin \theta_k} \right|^2, \quad (7a)$$

$$T_n(\theta_k) = \frac{2}{n(n+1)} \sum_{m=-n}^n \frac{(n-m)!}{(n+m)!} \left| \frac{dP_{nm}(\cos \theta_k)}{d\theta_k} \right|^2. \quad (7b)$$

The normalisation factor N is equal to one for plane waves, but assumes a different value for evanescent waves, as will be discussed below. For an incident plane wave it is easy to prove that $T_n = \Pi_n = 1$ for all multipolar orders n and angles θ_k with $\cos \theta_k \leq 1$, using the addition theorem of the associated Legendre polynomials. In this case the cross sections do not differ for s- and p-polarisation and (6) are the well-known results from standard Mie-theory.

For $\theta_i > \theta_c$, it follows from Snell's law that $\cos \theta_k > 1$, hence $\sin \theta_k$ becomes purely imaginary. The functions T_n, Π_n are listed in Table 1 for the lowest four multipolar orders. Because $\sin^2 \theta_k$ is now negative, $|\sin^2 \theta_k|$ in T_n and Π_n differs from $\sin^2 \theta_k$. Consequently, $T_n, \Pi_n > 1$, except $\Pi_1 = 1$. Furthermore, $T_n > \Pi_n$ for all n . As the component $k_M \sin \theta_k$ of the wavevector becomes imaginary, the magnitudes of the electromagnetic fields at distance d from the prism surface have exponentially decreased by a factor $\exp(-\kappa d)$ from their values at the prism surface where the attenuation constant is given by

$$\kappa = k_M \sin \theta_k = \frac{2\pi}{\lambda} (n_P^2 \sin^2 \theta_i - n_M^2)^{1/2}. \quad (8)$$

The energy flux given by the time-averaged Poynting vector is then not constant over the geometrical cross section of the

Table 1. Values of the functions $\Pi_n(\theta_k)$ and $T_n(\theta_k)$, defined in (7), for the lowest four multipolar orders. Here, $x = \cos \theta_k = (n_P/n_M) \sin \theta_i$ and $z = |\sin^2 \theta_k| - \sin^2 \theta_k$. It is $z = 0$ for plane waves, and $z = 2(x^2 - 1)$ for evanescent waves

| n | $\Pi_n(\theta_k)$ | $T_n(\theta_k)$ |
|-----|----------------------|----------------------------|
| 1 | 1 | $1+z$ |
| 2 | $1+z$ | $1+4x^2z$ |
| 3 | $1+2.5x^2z$ | $1+(15x^4-7.5x^2+1)z$ |
| 4 | $1+(7x^4-3.5x^2+1)z$ | $1+(56x^4-56x^2+14.5)x^2z$ |

sphere due to the exponential decrease of the fields. Therefore in the calculation of optical cross sections for evanescent-wave excitation the incident intensity I_0 has to be redefined. The corresponding quantity \tilde{I}_0 cannot be uniquely determined. Nevertheless it is reasonable to define cross sections in this case, as they represent particle-specific quantities and allow comparison to the case of plane waves. The corresponding problem has already been discussed for Gaussian beam illumination [7–9]. There the intensity in the center of the Gaussian beam waist was used for normalisation. In contrast to this we prefer to normalise to the total power incident on the particle, in order to avoid diverging efficiencies for large particles where the intensity of the evanescent wave at the center of the spherical particle is close to zero. The same normalisation was used by Lock [7] to define the extinction efficiency for the case of a Gaussian beam. It seems appropriate, however, to point out the limited meaning of any definition of cross sections for an excitation that varies significantly over the particle surface, as in all applications the scattered or absorbed power is the relevant quantity. For example, for large particle sizes the scattering of an evanescent wave arises only from a small part of the sphere and the definition of a cross section for the total particle becomes misleading.

As \tilde{I}_0 we choose the incident intensity, averaged over the cross-sectional area of the sample perpendicular to the Poynting vector of the evanescent wave.

$$\begin{aligned} \tilde{I}_0 &= \frac{1}{\pi a^2} \iint \langle \mathbf{S}_{\text{inc}} \rangle \cdot \mathbf{n} \, dA \\ &= I_0 \exp(-2\kappa d) \frac{n_P}{n_M} \sin \theta_i \frac{I_1(2\kappa a)}{\kappa a}, \end{aligned} \quad (9)$$

where $I_1(2\kappa a)$ is the modified Bessel function of order 1 with argument $2\kappa a$, for which the series expansion

$$\frac{I_1(2\kappa a)}{\kappa a} = 1 + \sum_{m=1}^{\infty} \frac{(\kappa a)^{2m}}{m!(m+1)!} \quad (10)$$

may be used. For a plane wave $\tilde{I}_0 = I_0$.

As the multipole expansions (2) and (4) for the incident and scattered fields are made in a coordinate system, whose origin coincides with the center of the sphere, the factor E_t in the multipole coefficients (3) and hence (5) has to be replaced by $E_t \exp(-\kappa d)$ for an evanescent wave. Therefore, for evanescent-wave excitation the factor $I_0 \exp(-2\kappa d)$ in (9) cancels out in the calculation of optical cross sections. The remaining factor,

$$N = \frac{n_P}{n_M} \sin \theta_i \frac{I_1(2\kappa a)}{\kappa a}, \quad (11)$$

is the normalisation factor which must be taken into account in the cross sections (6). For $\kappa a \ll 1$, i.e. very small particles compared to the wavelength of the incident light, it reduces to $N_0 = \frac{n_P}{n_M} \sin \theta_i$. The functions $N^{-1} T_n, N^{-1} \Pi_n$ have to be interpreted as weighting factors for the individual multipolar orders, relative to plane-wave excitation, in the cross sections for extinction and scattering of evanescent waves. Figure 2 displays the dependence of the size-independent weighting factors $\tilde{\Pi}_n = N_0^{-1} \Pi_n, \tilde{T}_n = N_0^{-1} T_n$ on the incident angle θ_i on a logarithmic scale for $n_P = 1.5, n_M = 1$. At and below the critical angle $\theta_c = 41.8^\circ$ all weighting factors are equal to

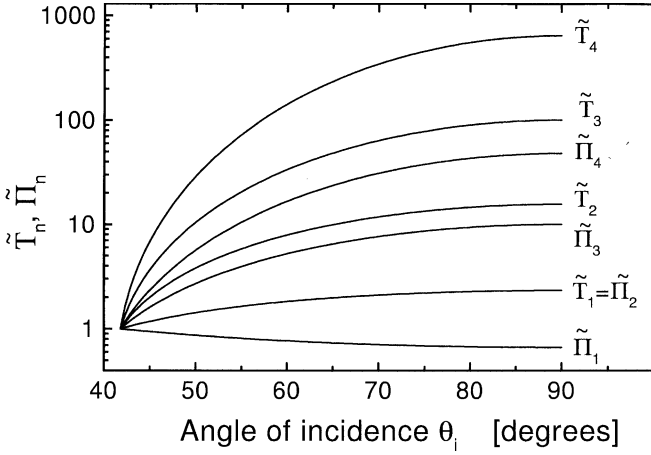


Fig. 2. Dependence of the functions $\tilde{\Pi}_n = N_0^{-1} \Pi_n$, $\tilde{T}_n = N_0^{-1} T_n$ on the angle of incidence θ_i for $n_p = 1.5$, $n_M = 1$. These functions are the weighting factors, relative to plane-wave excitation, of the individual multipolar contributions to the cross sections for extinction and scattering of evanescent waves by small spherical particles with $\kappa a \ll 1$ (compare the text)

one, as in this case the transmitted wave is a plane wave. The values of $\tilde{\Pi}_n$, \tilde{T}_n at large angles of incidence and for higher multipolar orders, on the other hand, are much larger than one. Therefore, the contributions of higher multipolar orders to scattering and extinction of evanescent waves are strongly enhanced relative to plane-wave excitation. For very small particles these contributions are limited, on the other hand, by the fact that the Mie coefficients a_n , b_n in (6) are then rapidly decreasing with increasing n . The decrease of a_n , b_n at sufficiently high orders insures convergence of the cross sections in (6) for all particle sizes, in spite of the strong increase of the functions $\tilde{\Pi}_n$, \tilde{T}_n with the order n in the case of evanescent waves. In addition, the normalisation factor N in the denominator quickly increases with particle size.

For sufficiently small particles, the relation $T_n > \Pi_n$ leads to $\sigma_{sca}^p > \sigma_{sca}^s$ for all wavelengths, as for such particles the absolute values of the Mie coefficients a_n for electric multipoles are larger than the coefficients b_n for magnetic multipoles to each order n . The same relation holds true for the extinction cross sections, as long as the real parts of the a_n exceed the real parts of the b_n . The fact that p-polarised evanescent waves scatter more strongly from small particles than s-polarised waves may be readily understood in the case of very small particles where the electric dipole approximation may be made. From the retarded potentials it follows that for an electric dipole induced in a small particle of an optically isotropic material in the monochromatic evanescent field \mathbf{E}_{ev} , of either p- or s-polarisation, the time-averaged radiated power is proportional to $\langle (\text{Re } \mathbf{E})^2 \rangle = \langle (\text{Im } \mathbf{E})^2 \rangle = \frac{1}{2} |\mathbf{E}_{ev}|^2$. For the p-polarised wave the latter quantity contains a factor $T_1 = |\sin \theta_k|^2 + \cos^2 \theta_k > 1$, which is missing in the case of s-polarisation. Furthermore, the factor does not appear in the expression for the power incident on the particle, to which the scattered power has to be normalised.

It seems appropriate to add a general comment on the polarization dependence of the optical cross sections for spherical particles, caused by the occurrence of the functions T_n and Π_n in (6). This polarisation dependence is due to the fact that p- and s-polarised evanescent waves are not related to each other by a simple rotation, i.e. a symmetry operation of

the sphere, in contrast to the corresponding plane waves: for p-polarised waves the electric field is rotating in the plane of incidence, due to the complex phase shift associated with total internal reflection, whereas for s-polarised waves it is oscillating perpendicular to it. It may be further noticed at this point that a polarisation dependence of the cross sections is already observed when the particle resides inside the prism, i.e. in the standing wave resulting from total internal reflection. The same holds for a particle in the standing wave in front of a metallic mirror where also a complex phase shift occurs in reflection. In both cases, however, the polarisation effects are much smaller than for evanescent waves.

2 Results for small silver particles

We have applied the theory outlined above to the scattering and extinction of light by small silver particles in front of the surface of a glass prism. Optical constants for silver were taken from [10]. Spectra for the extinction of particles with $2a = 10$ nm and $2a = 200$ nm are shown in Figs. 3 and 4, respectively. For the evanescent waves, $\theta_i = 60^\circ$, $n_p = 1.5$, and $n_M = 1$ is assumed (i.e. dispersion of n_p , n_M is neglected). In the analytical calculation, obviously, we neglected backscattering from the prism surface as well as multiple scattering. This is a reasonable assumption considering the low reflectivity of the glass surface.

Very small silver particles such as those of Fig. 3 exhibit the well-known dipolar surface plasmon resonance at around 365 nm. The shape of the extinction spectrum for evanescent waves is unchanged in this case compared to plane waves, and, as expected from the discussion above, the ratio of the cross sections for extinction as well as for scattering is for all wavelengths to a very good approximation given by $N_0^{-1} T_1$ (p-polarised evanescent wave) to 1 (plane wave) to $N_0^{-1} \Pi_1$ (s-polarised evanescent wave), with $\Pi_1 = 1$.

For larger particles, like those of Fig. 4 ($2a = 200$ nm), higher multipolar orders become important and are enhanced for evanescent waves as compared to plane waves. This leads

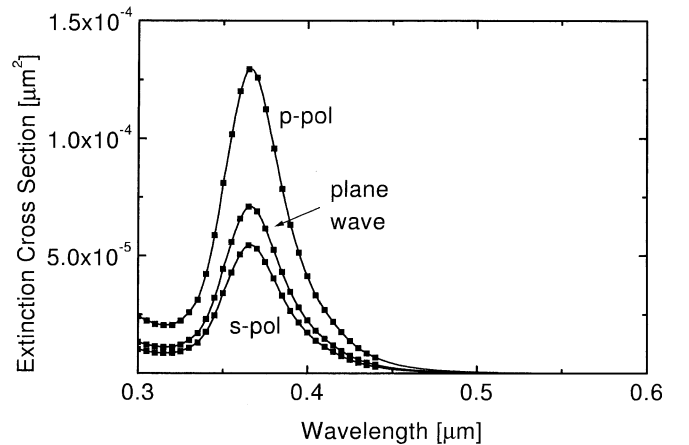


Fig. 3. Wavelength dependence of the cross sections for extinction of plane waves and evanescent waves by a spherical silver particle with $2a = 10$ nm. The *solid lines* are calculated using (6a,c) for evanescent waves and the formulae of standard Mie theory for plane waves, respectively. The *squares* indicate numerical results obtained by means of the multiple multipole (MMP) method. Thereby multiple scattering at the prism surface was neglected

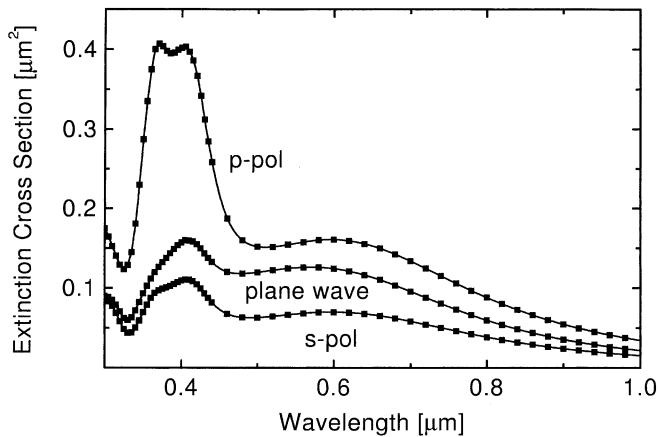


Fig. 4. Wavelength dependence of the cross sections for extinction of plane waves and evanescent waves by a spherical silver particle with $2a = 200$ nm. As in Fig. 3 the *solid lines* are the analytical results from (6a,c), and the *squares* indicate the numerical results obtained by means of the MMP method

to the structured spectra in Fig. 4, which are not simply in a constant ratio to each other any more. Figure 5 displays the decomposition of the extinction spectrum into the different multipolar contributions for p-polarised evanescent waves (Fig. 5a) and for plane waves (Fig. 5b), the numbers indicating the multipolar order. The strong enhancement of higher multipoles for evanescent-wave, as compared to plane-wave excitation, is evident. For example, the octupolar contribution to the spectrum of the large silver sphere in Fig. 5a can now clearly be resolved and leads to the double peak structure at short wavelengths. For s-polarization the higher multipoles are also enhanced with respect to plane-wave excitation but less than for p-polarization (compare Fig. 4 and Table 1). The scattering of spherical particles behaves qualitatively in the same way as the extinction (multipole decomposition for scattering cross sections not shown here), but higher multipolar contributions decrease faster with order n , as the squared absolute values of the Mie coefficients appearing in (6b,d) for

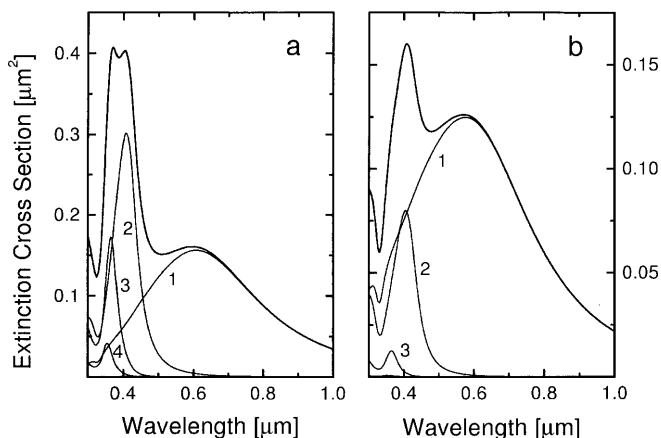


Fig. 5a,b. Decomposition of the extinction cross section into the individual multipole contributions for a silver particle with $2a = 200$ nm. **a** p-polarized evanescent wave. **b** Plane wave. The numbers indicate the order of the multipole, whose contribution to the total extinction cross section is shown. Results for s-polarized evanescent waves are not shown here, but are similar to those for p-polarization

the scattering cross sections decrease faster than their real parts, which determine the extinction, (6a,c).

We have finally applied a numerical technique for the calculation of electromagnetic fields, i.e. the multiple multipole (MMP) version [11] of the generalized multipole technique (GMT) [12], to the present case of scattering and extinction by small spherical particles to include the effect of multiple scattering. For comparison with the analytical results given above, backscattering from the surface, at which the evanescent wave is generated, was first neglected and the spatial distribution of electromagnetic field vectors and the Poynting vector of the scattered wave were calculated. The time-averaged Poynting vector was integrated numerically over a surface enclosing the particle to obtain the power of scattered light. Similarly, the excitation intensity was integrated numerically over the cross section of the sphere in order to obtain the normalisation factor for the cross sections. In Figs. 3 and 4 the symbols (full squares) indicate the numerically obtained results. Both methods are, of course, in excellent agreement for this simple geometry. We also obtained full agreement for various other absorbing and nonabsorbing particles and sizes not discussed here.

When the effect of backscattering from the prism was included in the calculation, we obtained the results shown in Fig. 6 for particles in contact with the surface of the prism. In Fig. 6, the extinction spectra for a p-polarised evanescent wave as well as for a plane wave are compared to those presented in Figs. 3 and 4. For the plane wave normal incidence from the prism side was assumed. From the curves in Fig. 6 it becomes obvious that the multiple scattering due to the prism surface leads to a significant redshift of peak positions. Moreover, in those parts of the spectra that are dominated by scattering, corresponding in the present spectra roughly to the wavelength range $\lambda > 0.4$ μm , the extinction cross section is enhanced, whereas it is diminished in those spectral regions where the absorption is the main contribution to extinction. The case of multiple scattering of plane waves for small particles on or near a surface has been treated analytically by various authors [13–18]. Similar to our results, a redshift and an enhancement of the scattering efficiency was observed. In [13–18] the plane wave was assumed, however, to be inci-

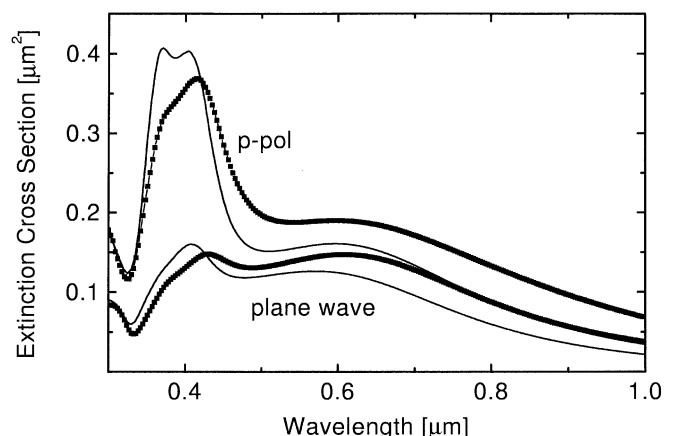


Fig. 6. Comparison of the extinction cross section spectra for a silver sphere with diameter $2a = 200$ nm in free space (*solid lines*) and on the glass prism (*squares*) for excitation with a plane wave (lower two curves) and a p-polarised evanescent wave (upper two curves)

dent from the side of the thinner medium. This is not directly comparable to the present case. A more detailed discussion of these effects will be given in a forthcoming paper.

3 Summary

In this paper, the theory of Chew et al. [4] and Liu et al. [5] for extinction and scattering of evanescent waves by spherical particles has been used to obtain total extinction and scattering cross sections. The cross sections have been defined for the case of evanescent waves, and an expression for the normalising integral has been given. Scattering and absorption of evanescent waves differ remarkably from scattering and absorption of plane waves in that the special properties of the evanescent wave lead to increased contributions of multipolar orders (n, m) with $n > 1$, which in turn lead to increased contributions of orders $n > 1$ in the expansion of the scattered wave. The results are polarisation-dependent cross sections, which are much larger for p-polarised light than for s-polarisation. The derived formalism was applied to silver particles of different sizes to compute optical cross sections at wavelengths between 300 nm and 1000 nm. The results show quantitatively the effects expected from the model, especially that higher multipolar orders n are weighted more strongly than for plane-wave excitation. It should be pointed out, however, that these effects are relevant not only in the special case of particles exhibiting plasma resonances, but more generally, for example in the case of the so-called morphological resonances.

We have further used the numerical multiple multipole (MMP) technique to test the analytical results and to take into account the influence of backscattering from the prism surface for particles on the glass prism surface. In comparison to our analytical results we have found excellent agreement.

Taking into account the prism surface finally leads to significant changes in the spectral dependence of the cross sections, which will be discussed in a forthcoming paper.

Acknowledgements. Financial support from the Deutsche Forschungsgemeinschaft (Innovationskolleg "Methods and Materials for the Nanometer Range") is gratefully acknowledged.

References

1. G. Mie: *Ann. Phys.* **25**, 377 (1908)
2. F. Zenhausern, Y. Martin, H.K. Wickramasinghe: *Science* **269**, 1083 (1995)
3. Y. Martin, F. Zenhausern, H.K. Wickramasinghe: *Appl. Phys. Lett.* **68**, 2475 (1996)
4. H. Chew, D.S. Wang, M. Kerker: *Appl. Opt.* **18**, 2679 (1979)
5. C. Liu, T. Kaiser, S. Lange, G. Schweiger: *Opt. Commun.* **117**, 521 (1995)
6. These changes are not related to the two different phase conventions in use for the associated Legendre polynomials
7. J.A. Lock: *J. Opt. Soc. Am. A* **12**, 929 (1995)
8. J.A. Lock, J.T. Hodges, G. Gouesbet: *J. Opt. Soc. Am. A* **12**, 2708 (1995)
9. G. Gouesbet, C. Letellier, G. Gréhan, J.T. Hodges: *Opt. Commun.* **125**, 137 (1996)
10. M. Quinten: *Z. Phys. B* **101**, 211 (1996)
11. Ch. Hafner: *The Generalized Multipole Technique for Computational Electromagnetics* (Artech House Books, ORT 1990)
12. A. Ludwig: *IEEE AP-S Newslett.* **31**, 40 (1989)
13. P.A. Bobbert, J. Vlieger: *Physica A* **137**, 207 (1986)
14. M.M. Wind, J. Vlieger, D. Bedeaux: *Physica A* **141**, 33 (1987)
15. G. Videen: *J. Opt. Soc. Am. A* **8**, 483 (1991)
16. G. Videen, M.G. Turner, V.J. Iafelice, W.S. Bickel, W.L. Wolfe: *J. Opt. Soc. Am. A* **10**, 118 (1993)
17. B.R. Johnson: *J. Opt. Soc. Am. A* **13**, 326 (1996)
18. E. Fucile, P. Denti, F. Borghese, R. Saija, O.I. Sindoni: *J. Opt. Soc. Am. A* **14**, 1505 (1997)